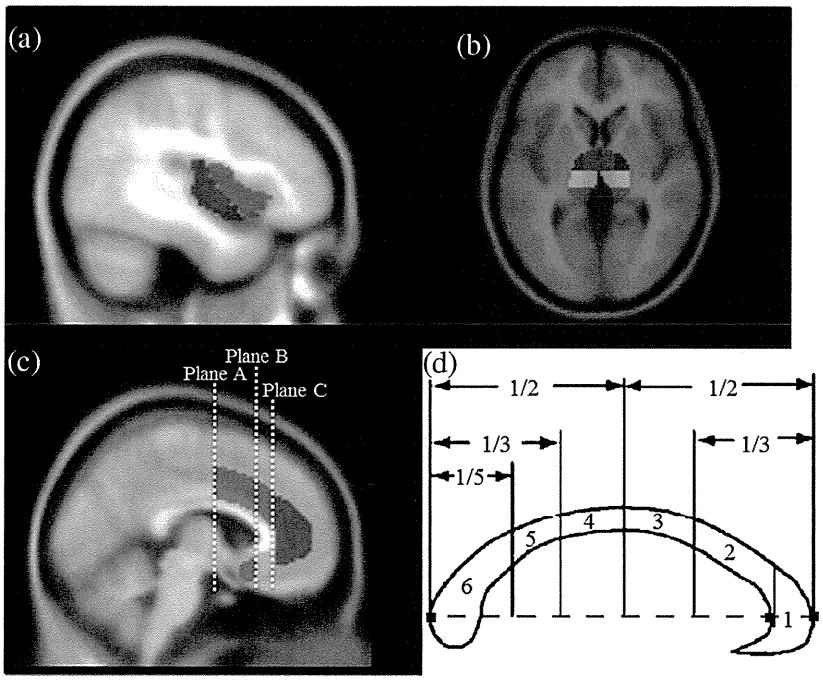

Fig. 1. The subclassification of the regions of interest (ROIs). (a) The insula was divided into two subregions: anterior (pink) and posterior (green). (b) The thalamus was divided into five subregions; the medial portions of the anterior (light blue) and central (purple) divisions, the lateral portions of the anterior (pink) and central divisions (green), and posterior divisions (red-orange). (c) The ACC was divided into four subregions; dorsal (red), rostral (blue), subcallosal (green), and subgenual subregions (pink). (d) Perpendiculars to this axis were drawn at specific arithmetic divisions, resulting in six callosal segments. The corpus callosum was divided into six subregions: genu (1), rostral body (2), anterior midbody (3), posterior midbody (4), isthmus (5) and splenium (6).

We entered FA values in bilateral anterior and posterior insulae, five thalamic subregions, four regions of the ACC, and six subregions of the corpus callosum, and volume data in bilateral anterior and posterior insulae, five thalamic subregions, and four anterior cingulate subregions, 3rd, 4th, and lateral ventricles as variables.

Discriminant functions were derived by stepwise methods after Wilks' method. The test was performed with the SPSS software ver. 17 (SPSS Japan, Tokyo). The stepwise selection criteria were determined by the overall multivariate *F*-value of each variable to test the differences between the patients with schizophrenia and those with MDD and to maximize the discriminant function between the groups. The enter-criterion was $F = 5$, and the remove-criterion was $F = 4$. An analysis was then performed to prospectively validate the statistical model, the linear discriminant function analysis, by successfully classifying the first two-group sample.

3. Results

The demographic and clinical data of the subjects are shown in Table 1, and the mean regional volumes and FA values of each ROIs were described in Table 2. The differences between the patients with schizophrenia and MDD were analyzed by two sample *t*-test. There was no significant difference in age, years of education, or whole brain volume between the schizophrenia and MDD groups in either sample.

Table 1
Demographic and clinical characteristics of the subjects.

Variable	(a) Exploration sample			(b) Validation sample		
	Schizophrenia	Major Depressive Disorder	*p* value	Schizophrenia	Major Depressive Disorder	*p* value
	Female ($n = 25$)	Female ($n = 25$)		Female ($n = 18$)	Female ($n = 16$)	
	Mean ± SD	Mean ± SD		Mean ± SD	Mean ± SD	
Age (years)	40.3 ± 10.6	42.3 ± 9.4	0.48	37.0 ± 8.7	41.5 ± 10.5	0.12
Education (years)	13.7 ± 2.5	14.5 ± 1.9	0.20	14.8 ± 2.5	14.5 ± 2.1	0.89
Duratin of illness (year)	17.9 ± 9.8	9.1 ± 9.1	0.002	15.6 ± 8.9	7.1 ± 5.9	0.012
Whole brain volume (liter)	1.10 ± 0.08	1.08 ± 0.08	0.42	1.13 ± 0.10	1.08 ± 0.10	0.20
Antipsychotic medication*	654.3 ± 547.1	8.0 ± 40.0	<0.001	427.0 ± 483.4	56.3 ± 225.0	0.006
Antidepressant medication#	0.0 ± 0.0	105.4 ± 143.0	0.001	0.0 ± 0.0	99.8 ± 103.1	0.001
Number of hospitalizations	3.5 ± 4.5	0.3 ± 0.5	0.002	1.8 ± 2.3	0.6 ± 1.0	0.023
HAM-D		12.2 ± 8.3			11.9 ± 7.2	
PANSS positive	14.6 ± 5.9			15.4 ± 6.1		
PANSS negative	16.8 ± 8.4			14.1 ± 4.8		
PANSS general	32.4 ± 13.5			29.6 ± 7.3		

HAM-D: Hamilton's rating scale for depression; PANSS: positive and negative syndrome scale; SD: standard deviation.
*: Chlorpromazine equivalent. #: Imipramine equivalent.

Table 2
Mean regional volume and fractional anisotropy of the subjects.

Region	Modality	Laterelity	(a) Exploration sample			(b) Validation sample		
			Schizophrenia	MDD	*p* value	Schizophrenia	MDD	*p* value
			Mean ± SD	Mean ± SD		Mean ± SD	Mean ± SD	
Corpus callosum 1	FA		0.49 ± 0.04	0.48 ± 0.04	0.52	0.51 ± 0.03	0.49 ± 0.04	0.09
Corpus callosum 2	FA		0.47 ± 0.05	0.49 ± 0.04	0.21	0.50 ± 0.05	0.50 ± 0.03	0.61
Corpus callosum 3	FA		0.43 ± 0.04	0.44 ± 0.04	0.37	0.45 ± 0.05	0.45 ± 0.04	0.69
Corpus callosum 4	FA		0.42 ± 0.04	0.42 ± 0.05	0.98	0.43 ± 0.05	0.42 ± 0.03	0.57
Corpus callosum 5	FA		0.43 ± 0.04	0.44 ± 0.05	0.32	0.45 ± 0.04	0.44 ± 0.03	0.55
Corpus callosum 6	FA		0.54 ± 0.03	0.55 ± 0.02	0.66	0.56 ± 0.03	0.56 ± 0.02	0.61
Anterior insula	FA	Left	0.22 ± 0.01	0.21 ± 0.01	0.04	0.21 ± 0.01	0.21 ± 0.01	0.91
		Right	0.21 ± 0.01	0.20 ± 0.01	0.03	0.20 ± 0.01	0.20 ± 0.01	0.92
	Volume	Left	0.38 ± 0.02	0.40 ± 0.03	0.05	0.37 ± 0.03	0.39 ± 0.02	0.06
		Right	0.39 ± 0.03	0.41 ± 0.03	0.01	0.38 ± 0.03	0.40 ± 0.03	0.05
Posterior insula	FA	Left	0.24 ± 0.02	0.23 ± 0.01	0.13	0.24 ± 0.01	0.23 ± 0.01	0.78
		Right	0.22 ± 0.01	0.22 ± 0.01	0.25	0.22 ± 0.01	0.22 ± 0.01	0.58
	Volume	Left	0.35 ± 0.03	0.36 ± 0.02	0.13	0.35 ± 0.02	0.36 ± 0.02	0.24
		Right	0.37 ± 0.03	0.37 ± 0.02	0.44	0.36 ± 0.02	0.37 ± 0.02	0.03
Anterolateral region of thalamus	FA	Left	0.46 ± 0.02	0.46 ± 0.02	0.22	0.46 ± 0.02	0.45 ± 0.02	0.07
		Right	0.46 ± 0.02	0.46 ± 0.02	0.88	0.46 ± 0.02	0.46 ± 0.02	0.56
	Volume	Left	0.09 ± 0.01	0.09 ± 0.01	0.41	0.08 ± 0.01	0.09 ± 0.01	0.01
		Right	0.09 ± 0.01	0.09 ± 0.01	0.32	0.09 ± 0.01	0.10 ± 0.01	0.00
Antero medial region of thalamus	FA	Left	0.32 ± 0.02	0.33 ± 0.02	0.59	0.33 ± 0.02	0.32 ± 0.02	0.20
		Right	0.32 ± 0.01	0.32 ± 0.02	0.75	0.34 ± 0.02	0.33 ± 0.02	0.31
	Volume	Left	0.22 ± 0.02	0.22 ± 0.02	0.29	0.21 ± 0.02	0.23 ± 0.03	0.00
		Right	0.23 ± 0.02	0.24 ± 0.02	0.03	0.22 ± 0.02	0.25 ± 0.03	0.00
Central lateral region of thalamus	FA	Left	0.41 ± 0.02	0.41 ± 0.02	0.56	0.41 ± 0.02	0.41 ± 0.02	0.75
		Right	0.40 ± 0.02	0.40 ± 0.02	0.81	0.40 ± 0.01	0.40 ± 0.02	0.49
	Volume	Left	0.14 ± 0.02	0.14 ± 0.01	0.66	0.13 ± 0.01	0.14 ± 0.01	0.02
		Right	0.17 ± 0.02	0.17 ± 0.01	0.45	0.17 ± 0.01	0.18 ± 0.02	0.02
Central medial region of thalamus	FA	Left	0.27 ± 0.02	0.28 ± 0.02	0.28	0.28 ± 0.02	0.27 ± 0.02	0.14
		Right	0.27 ± 0.02	0.27 ± 0.02	0.93	0.28 ± 0.02	0.27 ± 0.02	0.14
	Volume	Left	0.25 ± 0.02	0.26 ± 0.02	0.21	0.25 ± 0.02	0.27 ± 0.03	0.06
		Right	0.27 ± 0.02	0.28 ± 0.02	0.11	0.27 ± 0.02	0.29 ± 0.03	0.01
Posterior region of thalamus	FA	Left	0.27 ± 0.02	0.28 ± 0.02	0.08	0.28 ± 0.02	0.28 ± 0.01	0.89
		Right	0.27 ± 0.02	0.28 ± 0.02	0.10	0.28 ± 0.02	0.28 ± 0.01	0.84
	Volume	Left	0.22 ± 0.02	0.23 ± 0.02	0.46	0.22 ± 0.01	0.23 ± 0.02	0.06
		Right	0.25 ± 0.02	0.25 ± 0.02	0.80	0.24 ± 0.01	0.25 ± 0.02	0.03
Dorsoral ACC	FA	Left	0.26 ± 0.01	0.25 ± 0.01	0.19	0.25 ± 0.01	0.25 ± 0.01	0.73
		Right	0.31 ± 0.01	0.31 ± 0.01	0.75	0.31 ± 0.01	0.31 ± 0.01	0.53
	Volume	Left	0.37 ± 0.02	0.37 ± 0.02	0.17	0.37 ± 0.03	0.37 ± 0.02	0.69
		Right	0.32 ± 0.02	0.32 ± 0.02	0.56	0.32 ± 0.02	0.32 ± 0.02	0.90
Rostral ACC	FA	Left	0.19 ± 0.01	0.19 ± 0.01	0.23	0.19 ± 0.01	0.18 ± 0.01	0.04
		Right	0.24 ± 0.01	0.24 ± 0.01	0.16	0.24 ± 0.01	0.23 ± 0.01	0.32
	Volume	Left	0.41 ± 0.03	0.42 ± 0.03	0.41	0.42 ± 0.03	0.42 ± 0.02	0.84
		Right	0.38 ± 0.03	0.38 ± 0.03	0.35	0.38 ± 0.03	0.39 ± 0.02	0.31
Subcallosal ACC	FA	Left	0.22 ± 0.02	0.22 ± 0.02	0.93	0.22 ± 0.01	0.22 ± 0.02	0.26
		Right	0.29 ± 0.02	0.26 ± 0.02	0.00	0.28 ± 0.02	0.26 ± 0.03	0.01
	Volume	Left	0.40 ± 0.03	0.40 ± 0.03	0.36	0.39 ± 0.03	0.40 ± 0.03	0.25
		Right	0.35 ± 0.03	0.36 ± 0.03	0.28	0.36 ± 0.03	0.36 ± 0.03	0.48
Subgenual ACC	FA	Left	0.20 ± 0.02	0.21 ± 0.02	0.31	0.21 ± 0.02	0.20 ± 0.01	0.58
		Right	0.25 ± 0.03	0.24 ± 0.02	0.32	0.24 ± 0.02	0.24 ± 0.02	0.68
	Volume	Left	0.40 ± 0.03	0.41 ± 0.03	0.18	0.38 ± 0.03	0.40 ± 0.03	0.06
		Right	0.41 ± 0.02	0.42 ± 0.03	0.11	0.39 ± 0.03	0.41 ± 0.03	0.12
3rd ventricle	Volume		0.19 ± 0.05	0.17 ± 0.03	0.28	0.18 ± 0.04	0.18 ± 0.04	0.72
4th ventricle	Volume		0.18 ± 0.04	0.17 ± 0.03	0.27	0.18 ± 0.05	0.18 ± 0.05	0.99
Lateral ventricle	Volume		0.21 ± 0.12	0.19 ± 0.07	0.51	0.17 ± 0.07	0.18 ± 0.05	0.51

FA: fractional anisotropy; ACC: anterior cingulate cortex; MDD: major depressive disorder.

The stepwise discriminant analysis yielded a model in which three variables were selected. The obtained equation to calculate "discriminant score" is:

$$\text{Discriminant score} = 46.0 \times x - 39.4 \times y - 36.8 \times z + 6.9$$

where x is the FA value in the right subcallosal cingulate, y is the FA value in the posterior subregion of the thalamus, and z is the ratio of gray matter volume/whole brain volume in the right medial portion of the anterior thalamus. When the discriminant score is >0, it predicts that the patient has schizophrenia, and scores <0 predict MDD.

The use of these variables resulted in correct classification rates of 0.80 in schizophrenic patients and 0.76 in MDD patients in the first sample ($\chi^2 = 27.8$; df = 3; $p < 0.001$; Wilks' lambda = 0.55) (Fig. 2a). When the obtained discriminant model was applied to the second sample, the correct classification rates were 0.72 in schizophrenia and 0.88 in MDD groups (Fig. 2b).

4. Discussion

To our knowledge, this is the first attempt to produce a diagnostic tool to discriminate between schizophrenia and MDD based on structural MRI of the brain. Among the 31 ROIs located in the

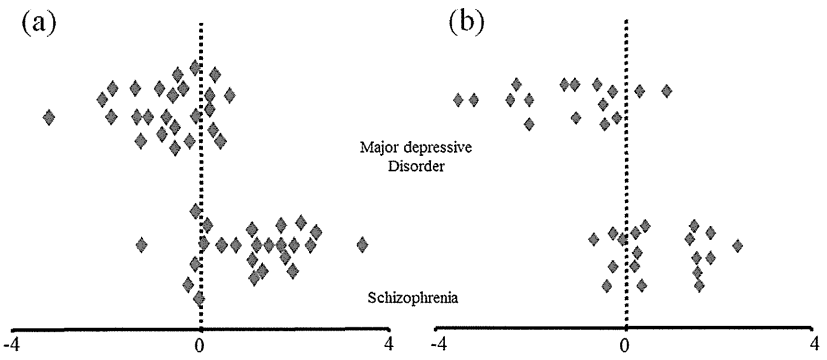

Fig. 2. Plot of discriminant scores in schizophrenic and MDD patients. (a) Discriminant scores of 25 schizophrenia patients and 25 MDD patients. (b) Discriminant scores of the second cohort of 18 schizophrenia patients and 16 MDD patients based on a linear discriminant function analysis between the original comparison samples.

thalami, ACC, insulae, corpus callosum, 3rd, 4th and lateral ventricles, three ROIs (i.e., the right subcallosal ACC, posterior subregion of the thalamus, and right medial portion of the anterior thalamus.) were selected to produce the discriminant model by the stepwise method. As for the correct classification rates, our results showed good classification rates of schizophrenia (0.80) and MDD (0.76) in the first exploration sample (0.90–1.00 = "excellent", 0.80–0.89 = "good", 0.70–0.79 = "fair", 0.60–0.69 = "poor", and 0.50–0.59 = "fail", according to Hanley and McNeil (1982) and Lasko et al. (2005)). Importantly, this discriminant model successfully classified the second sample of schizophrenia (0.72; fair), and MDD (0.88; good).

Several studies used high-resolution structural MRI scans as inputs to classification algorithms to distinguish between patients with schizophrenia and healthy volunteers, with reported accuracies ranging from 79% to 94% (Csernansky et al., 2004; Davatzikos et al., 2005; Fan et al., 2005; Kawasaki et al., 2007; Yoon et al., 2007). A few studies have assessed the feasibility of using FA and/or mean diffusivity (MD) maps in conjunction with automatic pattern recognition methods to differentiate between the two groups, and they correctly classified the patients with 75–94% accuracy (Ardekani et al., 2011; Caan et al., 2006; Caprihan et al., 2008).

Further, the accuracy of the structural neuroanatomy such as right subcallosal ACC and precuneus as a diagnostic marker for MDD was 67.6% (Costafreda et al., 2009). The relatively low accuracy rate in our study may have occurred because patients with mood disorders tend to share some neuroanatomical changes with schizophrenic patients (e.g. Meisenzahl et al., 2010).

The discriminant model in this study included the gray matter volume in the right medial portions of the anterior thalamus and FA in the right posterior subregion of the thalamus; these regions have been well known to be affected in schizophrenia, but not MDD (Honea et al., 2005; Konick and Friedman, 2001). On the other hand, previous neuroimaging studies showed the volume reduction of the subcallosal ACC in cases of MDD (Coryell et al., 2005; Costafreda et al., 2009; Pezawas et al., 2005). The discriminant model in this study also employed FA in the right subcallosal cingulate as a positive coefficient, and this is compatible with the preceding ones.

Limitation of the present study must be taken into account. First, this study included only female subjects. It is known that there were gender differences in brain morphology reported in MDD as well as schizophrenia patients (Suzuki et al., 2002; Takahashi et al., 2010), and that gender-difference effects on the course of progressive brain change in schizophrenia (Irle et al., 2011). In addition, some papers detect the gender-difference of brain configuration and the aging effect on the brain (Good et al., 2001; Pruessner et al., 2001). The correlative brain changes in male subjects need to be investigated separately. Second, there was a difference of mean duration of illness between the patient groups and we did not adjust the potential effects of age and duration of illness. It has been suggested that in schizophrenic patients, progressive brain changes occur that are rapid and diffuse compared with the aging effect of healthy subjects (Friedman et al., 2008; Mori et al., 2007). The effects of degenerative factors on the brain with MDD are not yet understood, and it is difficult to specify the duration of illness in MDD patient because MDD follows relapsing-remitting course. There is a need for systematic studies. It is difficult to adjust the factors that have different effects on the two groups respectively, so we tried to cope with these factors by balancing the mean age of the diagnostic groups.

In conclusion, our results suggest that schizophrenia and MDD have differential structural changes in the brain regions examined herein, and that a combination of such differences is useful to discriminate between patients with schizophrenia and those with MDD.

Role of funding sources

This study was supported by Health and Labor Sciences Research Grants (Comprehensive Research on Disability, Health, and Welfare) (M.O. and H.K.), Intramural Research Grant (24-11) for Neurological and Psychiatric Disorders of NCNP (M.O. and H.K.), "Understanding of molecular and environmental bases for brain health" carried out under the Strategic Research Program for Brain Sciences by the Ministry of Education, Culture, Sports, Science and Technology of Japan (H.K.).

Contributors

Miho Ota designed the study and wrote the first draft of the manuscript. Masanori Ishikawa collected data. Noriko Sato managed the analyses. Hiroaki Hori collected data. Daimei Sasayama collected data. Kotaro Hattori collected data. Toshiya Teraishi collected data. Takamasa Noda collected data. Satoko Obu collected data. Yasuhiro Nakata collected data. Teruhiko Higuchi managed the analyses. Hiroshi Kunugi managed the analyses. All authors contributed to and have approved the final manuscript.

Conflict of interest

All authors declare that they have no conflicts of interest.

Appendix A. Supplementary data

Supplementary data related to this article can be found at http://dx.doi.org/10.1016/j.jpsychires.2013.06.010.

References

American Psychiatric Association. DSM-IV Diagnostic and Statistical Manual of Mental Disorders. 4th ed. Washington, DC: APA; 1994.

American Psychiatric Association. Practice Guidelines for the Treatment of Patients with Schizophrenia. Washington, DC: American Psychiatric Press; 1997.

Andrade L, Caraveo-Anduaga JJ, Berglund P, Bijl RV, De Graaf R, Vollebergh W, et al. The epidemiology of major depressive episodes: results from the International Consortium of Psychiatric Epidemiology (ICPE) Surveys. International Journal of Methods in Psychiatric Research 2003;12(1):3–21.

Ardekani BA, Tabesh A, Sevy S, Robinson DG, Bilder RM, Szeszko PR. Diffusion tensor imaging reliably differentiates patients with schizophrenia from healthy volunteers. Human Brain Mapping 2011;32(1):1–9.

Arnone D, Cavanagh J, Gerber D, Lawrie SM, Ebmeier KP, McIntosh AM. Magnetic resonance imaging studies in bipolar disorder and schizophrenia: meta-analysis. British Journal of Psychiatry 2009;195(3):194–201.

Arnone D, McIntosh AM, Ebmeier KP, Munaf MR, Anderson IM. Magnetic resonance imaging studies in unipolar depression: systematic review and meta-regression analyses. European Neuropsychopharmacology 2012;22(1):1–16.

Ashburner J. A fast diffeomorphic image registration algorithm. Neuroimage 2007;38(1):95–113.

Bora E, Harrison BJ, Davey CG, Yücel M, Pantelis C. Meta-analysis of volumetric abnormalities in cortico-striatal-pallidal-thalamic circuits in major depressive disorder. Psychological Medicine 2012;42(4):671–81.

Brett, M., Anton, J.L., Valabregue, R., Poline, J.B., 2002. Region of interest analysis using an SPM toolbox [Abstract] presented at the 8th International Conference on Functional Mapping of the Human Brain. June 2–6, Sendai, Japan. Available on CD-ROM in Neuroimage, vol. 16, No. 2.

Buchsbaum MS, Someya T, Teng CY, Abel L, Chin S, Najafi A, et al. PET and MRI of the thalamus in never-medicated patients with schizophrenia. American Journal of Psychiatry 1996;153(2):191–9.

Caan MWA, Vermeer KA, van Vliet LJ, Majoie CBLM, Peters BD, den Heeten GJ, et al. Shaving diffusion tensor images in discriminant analysis: a study into schizophrenia. Medical Image Analysis 2006;10(6):841–9.

Caprihan A, Pearlson GD, Calhoun VD. Application of principal component analysis to distinguish patients with schizophrenia from healthy controls based on fractional anisotropy measurements. Neuroimage 2008;42(2):675–82.

Coryell W, Nopoulos P, Drevets W, Wilson T, Andreasen NC. Subgenual prefrontal cortex volumes in major depressive disorder and schizophrenia: diagnostic specificity and prognostic implications. American Journal of Psychiatry 2005;162(9):1706–17012.

Costafreda SG, Chu C, Ashburner J, Fu CH. Prognostic and diagnostic potential of the structural neuroanatomy of depression. PLoS One 2009;4(7):e6353.

Crespo-Facorro B, Kim JJ, Andreasen NC, O'Leary DS, Bockholt J, Magnotta V. Insular cortex abnormalities in schizophrenia: a structural magnetic resonance imaging study of first-episode patients. Schizophrenia Research 2000;46(1):35–43.

Csernansky JG, Schindler MK, Splinter NR, Wang L, Gado M, Selemon LD, et al. Abnormalities of thalamic volume and shape in schizophrenia. American Journal of Psychiatry 2004;161(5):896–902.

Davatzikos C, Shen D, Gur RC, Wu X, Liu D, Fan Y, et al. Whole-brain morphometric study of schizophrenia revealing a spatially complex set of focal abnormalities. Archives of General Psychiatry 2005;62(11):1218–27.

Fan Y, Shen D, Davatzikos C. Classification of structural images via high-dimensional image warping, robust feature extraction, and SVM. Medical Image Computing and Computer-Assisted Intervention 2005;Pt 1:1–8.

Friedman JI, Tang C, Carpenter D, Buchsbaum M, Schmeidler J, Flanagan L, et al. Diffusion tensor imaging findings in first-episode and chronic schizophrenia patients. American Journal of Psychiatry 2008;165(8):1024–32.

Glahn DC, Laird AR, Ellison-Wright I, Thelen SM, Robinson JL, Lancaster JL, et al. Meta-analysis of gray matter anomalies in schizophrenia: application of anatomic likelihood estimation and network analysis. Biological Psychiatry 2008;64(9):774–81.

Good CD, Johnsrude I, Ashburner J, Henson RNA, Friston KJ, Frackowiak RSJ. Cerebral asymmetry and the effect of sex and handedness on brain structure: a voxel-based morphometric analysis of 465 normal adult human brains. Neuroimage 2001;14(3):685–700.

Hamilton M. A rating scale of depression. Journal of Neurology, Neurosurgery and Psychiatry 1960;23(1):56–62.

Hanley J, McNeil B. The meaning and use of the area under a receiver operating characteristic (ROC) curve. Radiology 1982;143(1):29–36.

Honea R, Crow TJ, Passingham D, Mackay CE. Regional deficits in brain volume in schizophrenia: a meta-analysis of voxel-based morphometry studies. American Journal of Psychiatry 2005;162(12):2233–45.

Inagaki A, Inada T, Fujii Y, Yagi G. Equivalent dose of psychotropics. Tokyo: Seiwa Shoten; 1999.

Irle E, Lange C, Ruhleder M, Exner C, Siemerkus J, Weniger G. Hippocampal size in women but not men with schizophrenia relates to disorder duration. Psychiatry Research 2011;192(3):133–9.

Jiang H, van Zijil PC, Kim J, Pearlson GD, Mori S. DtiStudio: resource program for diffusion tensor computation and fiber bundle tracking. Computer Methods and Programs in Biomedicine 2006;81(2):106–16.

Kawasaki Y, Suzuki M, Kherif F, Takahashi T, Zhou SY, Nakamura K, et al. Multivariate voxel-based morphometry successfully differentiates schizophrenia patients from healthy controls. Neuroimage 2007;34(1):235–42.

Kay SR, Opler LA, Fiszbein A. Positive and Negative Syndrome Scale (PANSS) manual. Schizophrenia Bulletin 1987;13(2):261–76.

Kollias CT, Kontaxakis VP, Havaki-Kontaxaki BJ, Stamouli S, Margariti M, Petridou E. Association of physical and social anhedonia with depression in the acute phase of schizophrenia. Psychopathology 2008;41(6):365–70.

Konick LC, Friedman L. Meta-analysis of thalamic size in schizophrenia. Biological Psychiatry 2001;49(1):28–38.

Lasko T, Bhagwat J, Zou K, Ohno-Machado L. The use of receiver operating characteristic curves in biomedical informatics. Journal of Biomedical Informatics 2005;38(5):404–15.

Leonard CM, Kuldau JM, Breier JI, Zuffante PA, Gautier ER, Heron DC, et al. Cumulative effect of anatomical risk factors for schizophrenia: an MRI study. Biological Psychiatry 1999;46(3):374–82.

Makris N, Goldstein J, Kennedy D, Hodge S, Caviness V, Faraone S, et al. Decreased volume of left and total anterior insular lobule in schizophrenia. Schizophrenia Research 2006;83(2-3):155–71.

Maldjian JA, Laurienti PJ, Kraft RA, Burdette JH. An automated method for neuroanatomic and cytoarchitectonic atlas-based interrogation of fMRI data sets. Neuroimage 2003;19(3):1233–9.

Maldjian JA, Laurienti PJ, Burdette JH. Precentral gyrus discrepancy in electronic versions of the Talairach atlas. Neuroimage 2004;21(1):450–5.

McCormick LM, Ziebell S, Nopoulos P, Cassell M, Andreasen NC, Brumm M. Anterior cingulate cortex: an MRI-based parcellation method. Neuroimage 2006;32(3):1167–75.

Meisenzahl EM, Seifert D, Bottlender R, Teipel S, Zetzsche T, Jäger M, et al. Differences in hippocampal volume between major depression and schizophrenia: a comparative neuroimaging study. European Archives of Psychiatry and Clinical Neuroscience 2010;260(2):127–37.

Mitelman SA, Nikiforova YK, Canfield EL, Hazlett EA, Brickman AM, Shihabuddin L, et al. A longitudinal study of the corpus callosum in chronic schizophrenia. Schizophrenia Research 2009;114(1-3):144–53.

Mori T, Ohnishi T, Hashimoto R, Nemoto K, Moriguchi Y, Noguchi H, et al. Progressive changes of white matter integrity in schizophrenia revealed by diffusion tensor imaging. Psychiatry Research 2007;154:133–45.

Nakamura M, Salisbury DF, Hirayasu Y, Bouix S, Pohl KM, Yoshida T, et al. Neocortical gray matter volume in first-episode schizophrenia and first-episode affective psychosis: a cross-sectional and longitudinal MRI study. Biological Psychiatry 2007;62:773–83.

Ota M, Sato N, Ishikawa M, Hori H, Sasayama D, Hattori K, et al. Discrimination of schizophrenic females from healthy women using multiple structural brain measures obtained with voxel-based morphometry. Psychiatry and Clinical Neurosciences 2012;66(7):611–7.

Pruessner JC, Collins DL, Pruessner M, Evans AC. Age and gender predict volume decline in the anterior and posterior hippocampus in early adulthood. Journal of Neuroscience 2001;21(1):194–200.

Pernet C, Andersson J, Paulesu E, Demonet JF. When all hypotheses are right: a multifocal account of dyslexia. Human Brain Mapping 2009;30(7):2278–92.

Pezawas L, Meyer-Lindenberg A, Drabant EM, Verchinski BA, Munoz KE, Kolachana BS, et al. 5-HTTLPR polymorphism impacts human cingulate-amygdala interactions: a genetic susceptibility mechanism for depression. Nature Neuroscience 2005;8(6):828–34.

Saha S, Chant D, Welham J, McGrath J. A systematic review of the prevalence of schizophrenia. PLoS Medicine 2005;2(5):e141.

Sexton CE, Mackay CE, Ebmeier KP. A systematic review of diffusion tensor imaging studies in affective disorders. Biological Psychiatry 2009;66(9):814–23.

Suzuki M, Nohara S, Hagino H, Kurokawa K, Yotsutsuji T, Kawasaki Y, et al. Regional change in gray and white matter in patients with schizophrenia demonstrated with voxel-based analysis of MRI. Schizophrenia Research 2002;55(1-2):41–54.

Takahashi T, Yücel M, Lorenzetti V, Tanino R, Whittle S, Suzuki M, et al. Volumetric MRI study of the insular cortex in individuals with current and past major depression. Journal of Affective Disorders- 2010;121(3):231–8.

Takayanagi Y, Kawasaki Y, Nakamura K, Takahashi T, Orikabe L, Toyoda E, et al. Differentiation of first-episode schizophrenia patients from healthy controls using ROI-based multiple structural brain variables. Progress in Neuropsychopharmacology and Biological Psychiatry 2010;34(1):10–7.

Wakana S, Jiang H, Nagae-Poetscher LM, van Zijl PC, Mori S. Fiber tract-based atlas of human white matter anatomy. Radiology 2004;230(1):77–87.

White T, Nelson M, Lim KO. Diffusion tensor imaging in psychiatric disorders. Topics in Magnetic Resonance Imaging 2008;19(2):97–109.

Witelson SF. Hand and sex differences in the isthmus and genu of the human corpus callosum. Brain 1989;112(Pt 3):799–835.

Yoon U, Lee JM, Im K, Shin YW, Cho BH, Kim IY, et al. Pattern classification using principal components of cortical thickness and its discriminative pattern in schizophrenia. Neuroimage 2007;34(4):1405–15.

ARTICLE IN PRESS
SCHRES-05759; No of Pages 6
Schizophrenia Research xxx (2014) xxx–xxx
Contents lists available at ScienceDirect
Schizophrenia Research
journal homepage: www.elsevier.com/locate/schres

Pseudo-continuous arterial spin labeling MRI study of schizophrenic patients

Miho Ota [a,*], Masanori Ishikawa [b], Noriko Sato [c], Mitsutoshi Okazaki [b], Norihide Maikusa [d], Hiroaki Hori [a], Kotaro Hattori [a], Toshiya Teraishi [a], Kimiteru Ito [c], Hiroshi Kunugi [a]

[a] Department of Mental Disorder Research, National Institute of Neuroscience, National Center of Neurology and Psychiatry, 4-1-1, Ogawa-Higashi, Kodaira, Tokyo 187-8502, Japan
[b] Department of Psychiatry, National Center of Neurology and Psychiatry, 4-1-1, Ogawa-Higashi, Kodaira, Tokyo 187-8502, Japan
[c] Department of Radiology, National Center of Neurology and Psychiatry, 4-1-1, Ogawa-Higashi, Kodaira, Tokyo 187-8502, Japan
[d] Department of Imaging Neuroinformatics, Integrative Brain Imaging Center, National Center of Neurology and Psychiatry, 4-1-1, Ogawa-Higashi, Kodaira, Tokyo 187-8502, Japan

ARTICLE INFO

Article history:
Received 14 May 2013
Received in revised form 16 December 2013
Accepted 16 January 2014
Available online xxxx

Keywords:
Biological parametric mapping
Cerebral blood flow
Diffeomorphic anatomical registration using exponentiated Lie algebra
Pseudo-continuous arterial spin labeling
Schizophrenia
Tract-based spatial statistics

ABSTRACT

Arterial spin labeling (ASL) magnetic resonance imaging (MRI) is a novel noninvasive technique that can measure regional cerebral blood flow (rCBF). To our knowledge, few studies have examined rCBF in patients with schizophrenia by ASL-MRI. Here we used pseudo-continuous ASL (pCASL) to examine the structural and functional imaging data in schizophrenic patients, taking the regional cerebral gray matter volume into account. The subjects were 36 patients with schizophrenia and 42 healthy volunteers who underwent 3-tesla MRI, diffusion tensor imaging (DTI), and pCASL. We evaluated the gray matter volume imaging, DTI, and pCASL imaging data in a voxel-by-voxel statistical analysis. The schizophrenia patients showed reduced rCBF in the left prefrontal and bilateral occipital cortices compared to the healthy volunteers. There was a significant reduction of gray matter volume in the left inferior frontal cortex in the schizophrenia patients. With respect to the fractional anisotropy (FA) values in the DTI, there were significant FA reductions in the left superior temporal, left external capsule, and left inferior prefrontal regions in the patients compared to the controls.
Conclusion: Our pCASL study with partial volume effect correction together with volumetry and DTI data demonstrated hypoactivity in the left prefrontal area beyond structural abnormalities in schizophrenia patients. There were also hypofunction areas in bilateral occipital cortices, although structural abnormalities were not apparent.

1. Introduction

Schizophrenia is a complex disorder characterized by symptoms such as hallucinations, delusions, disorganized communication, poor planning, reduced motivation, and blunted affect. Structural brain abnormalities, such as ventricular enlargement, total brain volume deficits, and deficits in brain volume within the frontal, temporal, and parietal regions have been consistently reported in people with schizophrenia (reviewed in Shenton et al., 2001; Honea et al., 2005; Kanaan et al., 2005; Kubicki et al., 2007). Previous studies using nuclear medicine techniques such as single photon emission computed tomography (SPECT) showed significant reductions of regional cerebral blood flow (rCBF) in the frontal, parietal, and temporal regions of people with schizophrenia (Vita et al., 1995; Kanahara et al., 2009).

Arterial spin labeling (ASL) magnetic resonance imaging (MRI) is a novel noninvasive (i.e., non-radioactive) technique that can measure rCBF by taking advantage of arterial water as a freely diffusible tracer. A few studies have shown that ASL is useful to detect functional abnormalities of the brain in schizophrenic individuals (Horn et al., 2009; Scheef et al., 2010; Pinkham et al., 2011; Walther et al., 2011). Some of these studies showed the rCBF reduction in the frontal and parietal regions (Scheef et al., 2010; Pinkham et al., 2011; Walther et al., 2011), occipital region (Pinkham et al., 2011), and the temporal region and cingulum (Scheef et al., 2010; Walther et al., 2011); however, another study found no significant difference between patients and controls (Horn et al., 2009). Additionally, the limited spatial resolution of ASL images precludes exact rCBF measurements because the partial volume effects on ASL cause an underestimation of activity in small structures of the brain. Since many schizophrenia patients have altered brain structures as described above, their rCBF images are likely to be influenced by the partial volume effect. To our knowledge, however, no ASL study has thus far taken account of the partial volume effect.

In this study, we examined differences in rCBF between patients with schizophrenia and healthy controls by a recently developed method, pseudo-continuous ASL (pCASL). pCASL combines the advantages of pulsed ASL (PASL) and continuous ASL (CASL); PASL is less costly and CASL has a higher signal-to-noise ratio. Previously we demonstrated that pCASL could show the change of rCBF in multiple

* Corresponding author at: Department of Mental Disorder Research, National Institute of Neuroscience, National Center of Neurology and Psychiatry, 4-1-1, Ogawa-Higashi, Kodaira, Tokyo 187-8502, Japan. Tel.: +81 42 341 2712; fax: +81 42 346 2094.
E-mail address: ota@ncnp.go.jp (M. Ota).

0920-9964/$ – see front matter © 2014 Elsevier B.V. All rights reserved.
http://dx.doi.org/10.1016/j.schres.2014.01.035

sclerosis in a similar way as SPECT (Ota et al., 2013). Simultaneously, we also evaluated structural differences between the two groups by a three-dimensional volumetric acquisition of T1-weighted sequences and diffusion tensor imaging (DTI).

2. Materials and methods

2.1. Subjects

The subjects were 36 patients with schizophrenia and 42 age- and gender-matched healthy subjects. A consensus diagnosis by at least two psychiatrists was made according to the Diagnostic and Statistical Manual of Mental Disorders, 4th ed. (DSM-IV) criteria (American Psychiatric Association, 1994), on the basis of unstructured interviews and information from medical records. Twenty-one of the 36 patients were inpatients and were admitted to an acute psychiatric ward of the National Center of Neurology and Psychiatry Hospital, Japan. Thirty-four of the 36 patients were chronic cases, and the remaining two patients were experiencing first-episode schizophrenia. The psychopathological state of all of the schizophrenic patients was assessed with the Positive and Negative Syndrome Scale (PANSS) (Kay et al., 1987).

Controls were recruited from the community through local magazine advertisements and our website announcement. These participants were interviewed for enrollment by a research psychiatrist using the Japanese version of the Mini-International Neuropsychiatric Interview (Sheehan et al., 1998; Otsubo et al., 2005). Participants were excluded if they had a prior medical history of central nervous system disease or severe head injury, or if they met the criteria for substance abuse or dependence. Those individuals who demonstrated a history of psychiatric illness or contact with psychiatric services were excluded from the control group. Daily doses of antipsychotics, including depot antipsychotics, were converted to chlorpromazine equivalents using published guidelines (American Psychiatric Association, 1997; Inagaki et al., 1999).

After the study was explained to each participant, his or her written informed consent was obtained for participation in the study. This study was approved by the ethics committee of the National Center of Neurology and Psychiatry, Japan.

2.2. MRI data acquisition and processing

Imaging was performed on a 3-tesla MR system (Philips Medical Systems, Best, The Netherlands). High spatial resolution, 3-dimensional (3D) T1-weighted images were used for the morphometric study. 3D T1-weighted images were acquired in the sagittal plane (repetition time [TR]/echo time [TE], 7.18/3.46; flip angle, 10°; effective section thickness, 0.6 mm; slab thickness, 180 mm; matrix, 384 × 384; field of view [FOV], 261 × 261 mm; number of signals acquired, 1, yielding 300 contiguous slices through the brain.

DTI was performed in the axial plane (TR/TE, 5760/62 ms; matrix, 80 × 80; FOV, 240 × 240 mm; 60 continuous transverse slices; slice thickness 3 mm with no interslice gap). To enhance the signal-to-noise ratio, acquisition was performed two times. Diffusion was measured along 15 non-collinear directions using a diffusion-weighted factor *b* in each direction for 1000 s/mm2, and one image was acquired without using any diffusion gradient. The imaging parameters for all of the pCASL experiments were identical: single-shot gradient-echo echo planar imaging (EPI) in combination with parallel imaging imaging (SENSE factor 2.0), TR = 4000 ms, TE = 12 ms, matrix = 64 × 64, FOV = 240 × 240, voxel size = 3.75 × 3.75 mm, 20 slices acquired in ascending order, slice thickness = 7 mm, 1-mm gap between slices, labeling duration = 1650 ms, post-spin labeling delay = 1520 ms, time interval between consecutive slice acquisitions = 32.0 ms, RF duration = 0.5 ms, pause between RF pulses = 0.5 ms, labeling pulse flip angle = 18°, bandwidth = 3.3 kHz/pixel, echo train length = 35. Thirty-two pairs of control/label images were acquired and averaged. The scan duration was 4 min and 24 s. For measurement of the magnetization of arterial blood and also for segmentation purposes, an EPI M0 image was obtained separately with the same geometry and the same imaging parameters as the pCASL without labeling.

2.3. Postprocessing of the ASL data

Because the pCASL and M0 images were acquired separately, the image signal intensities of both were corrected for data scaling. Corrected data were transferred to a workstation and analyzed by using ASLtbx software (Wang et al., 2008) running on statistical parametric mapping 5 (SPM5). For the rCBF calculations, we added the attenuation correction for the transversal relaxation rate of gray matter to the original equation. Details of this process are described elsewhere (Ota et al., 2013). The parameters used in the present study were: longitudinal relaxation time of blood = 1664 ms (Lu et al., 2004), labeling efficiency = 0.85 (Aslan et al., 2010), transversal relaxation time of gray matter (assumed to be 44.2 ms; Cavuşoğlu et al., 2009), and blood/tissue water partition coefficient = 0.9 g/ml (Wang et al., 2005).

The mean rCBF image derived by using the ASLtbx software contained some patchy noise, and thus we used a median filter (a nonlinear digital filtering technique). In median filtering, the neighboring pixels are ranked according to their intensity, and the median value becomes the new value for the central pixel. Since the slice gap that we used was somewhat large, simple 2D median filtering (3 voxels × 3 voxels) was used. To evaluate rCBF on a voxel-by-voxel basis, we normalized the mean rCBF images to the standard space. First, each individual 3D-T1 image was coregistered and resliced to its own M0 image. Next, the coregistered 3D-T1 image was normalized to the "avg152T1" image regarded as the anatomically standard image. Finally, the transformation matrix was applied to the mean rCBF images treated with the median filter. The spatially normalized images were resliced with a final voxel size of approx. 4 × 4 × 8 mm. Each map was then spatially smoothed with a 4-mm full-width at half-maximum Gaussian kernel in order to decrease spatial noise and compensate for the inexactitude of normalization.

2.4. Diffeomorphic anatomical registration using an exponentiated lie algebra (DARTEL) analysis

A preprocessing step of voxel based morphometry (VBM) in SPM was improved with the DARTEL (diffeomorphic anatomical registration using exponentiated lie) registration method (Ashburner, 2007). Calculations and image matrix manipulations were performed by using SPM8 working on a Matlab 7.0 (Math Works, Natick, MA, USA). The brain images were segmented, normalized, and modulated by using a set of group-specific templates. The gray matter probability values were then smoothed by using a 12-mm full-width at half-maximum Gaussian kernel.

2.5. Tract-based spatial statistics (TBSS) analysis

We evaluated the fractional anisotropy (FA) images by the processing technique known as tract-based spatial statistics (TBSS) analysis (Smith et al., 2006). TBSS is available as part of the FSL 4.1 software package (Smith et al., 2004). TBSS projects each subject's aligned FA image to the FMRIB58_FA template, which is supplied with FSL, onto the binary mask called the "skeleton image" derived from the mean FA image limited the FA value to >0.2. This results in skeletonized FA data. It is this file that is used for the voxelwise statistics.

Please cite this article as: Ota, M., et al., Pseudo-continuous arterial spin labeling MRI study of schizophrenic patients, Schizophr. Res. (2014), http://dx.doi.org/10.1016/j.schres.2014.01.035

Table 1
Demographic and clinical characteristics of the study participants.

	Healthy volunteers	Schizophrenia patients	*p* value
Male/female	21/21	17/19	0.81
Age (year)	37.9 ± 13.0	39.8 ± 12.6	0.52
Education (year)	14.7 ± 2.5	13.9 ± 3.2	0.27
Inpatient/outpatient		21/15	
First-episode/second and later		2/34	
Duration of illness (year)		16.8 ± 11.3	
Antipsychotic medication (mg/day)*		604.8 ± 459.2	
PANSS total		61.8 ± 19.3	
Positive		15.3 ± 5.6	
Negative		14.9 ± 6.2	
General		31.7 ± 10.4	

PANSS; positive and negative syndrome scale.
*: Chlorpromazine equivalent.

2.6. Statistical analysis

Statistical analyses were performed by using SPM5 software. Differences in gray matter volume and rCBF between the patients and controls were assessed by using the subjects' age, gender, and education years as nuisance variables. We evaluated the gray matter volume, controlling for the whole brain volume. When the rCBF differences were analyzed, we added the regional gray matter volume derived from the individual segmented gray matter volume image as a covariate using Biological Parametric Mapping (BPM) (Casanova et al., 2007). Since the gray matter volume values are different in various brain regions, each voxel of the rCBF image was adjusted by gray matter volume in the BPM analysis. Only differences that met the following criteria were deemed significant. In this case, a seed level of $p < 0.001$ (uncorrected) and a cluster level of $p < 0.05$ (uncorrected) were adopted. We next examined the possible correlation between rCBF and PANSS subscales of the subjects controlling for age, gender and regional gray matter volume by multiple regression model. The same p values shown above were regarded as significant. Skeletonized FA data were analyzed to identify differences between the two groups, controlling for age, gender and education years using the FSL "Threshold-Free Cluster Enhancement (TFCE)" option in "randomize" with 10 000 permutations (Nichols and Holmes, 2002; Smith and Nichols, 2009). The significance level was set at the p-value of less than 0.05 with the family-wise error (FWE) rate correction for multiple comparisons.

3. Results

The demographic and clinical characteristics of the participants are shown in Table 1. There was no significant difference in age, gender, or education years between the patients with schizophrenia and controls.

We evaluated the gray matter volume differences by performing a DARTEL analysis. A significant gray matter volume reduction was found in the left inferior prefrontal cortex in the patients compared to the controls (Fig. 1). No significant increase was detected in the patients.

We then examined the possible differences in rCBF between the two groups by using SPM5 with regional gray matter volume, age, gender, and education years as nuisance variables. There was a significant rCBF reduction in the left inferior prefrontal cortex and bilateral occipital cortices in the patients compared to the controls (Fig. 2). No significant increase in rCBF was detected in any region in the patients. Using the Wake Forest University (WFU) PickAtlas (Maldjian et al., 2003), we then performed small volume corrections (SVCs) for inferior frontal gyri defined by the Automated Anatomical Labeling (AAL) atlas (Tzourio-Mazoyer et al., 2002). For this SVC analysis, FWE-corrected voxel level threshold of $p < 0.05$ was applied to account for multiple comparisons of the results (Table 2).

As for the relationships between the clinical variables and rCBF, we could not detect any significant correlations, however we found a nominal negative correlation between PANSS negative scale and rCBF in bilateral superior temporal gyri, left inferior prefrontal cortex, and left thalamus at trend level (Fig. 3).

When we examined the DTI results, we observed significant reductions of FA values in the left superior temporal region, left external capsule, and left inferior frontal region in the schizophrenia patients compared to the controls (Fig. 4). No significant increase in FA was detected in any region in the patients.

4. Discussion

To our knowledge, this is the first study of ASL-based rCBF changes in schizophrenic patients that took the regional gray matter volume into

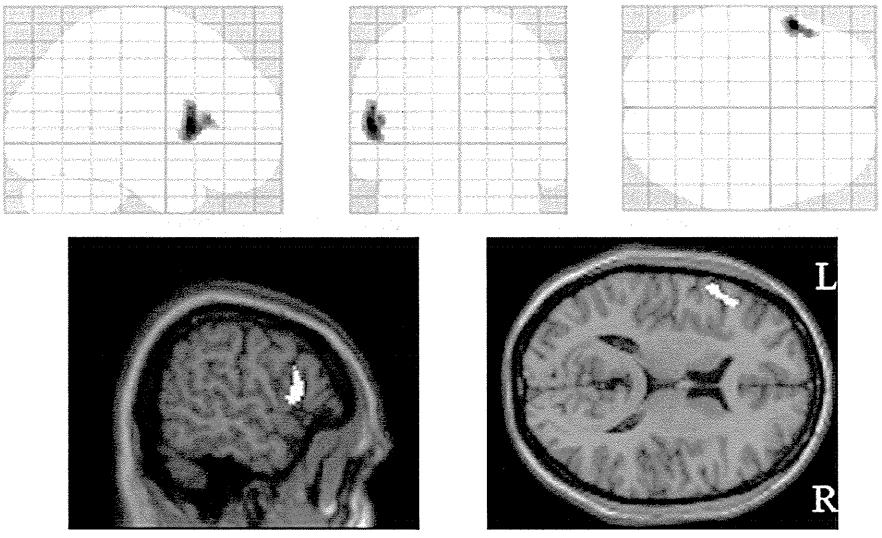

Fig. 1. Regional gray matter volume changes in schizophrenia. There were significant reductions of gray matter volume in the left prefrontal cortex of the patients with schizophrenia ($p < 0.001$, uncorrected). L: left, R: right.

Please cite this article as: Ota, M., et al., Pseudo-continuous arterial spin labeling MRI study of schizophrenic patients, Schizophr. Res. (2014), http://dx.doi.org/10.1016/j.schres.2014.01.035

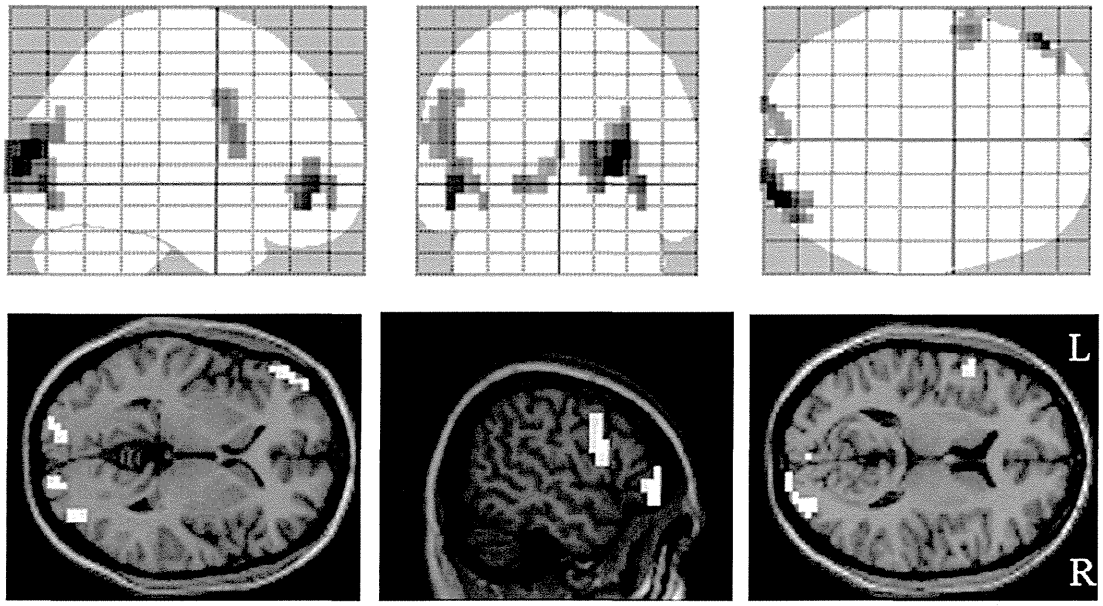

Fig. 2. Regional cerebral blood flow (rCBF) changes in schizophrenia. There were significant reductions of rCBF in the left prefrontal cortex and bilateral occipital cortices of the patients with schizophrenia ($p < 0.001$, uncorrected). L: left, R: right.

account. Using the pCASL method, we found that there were significant rCBF reductions in the left inferior prefrontal cortex and bilateral occipital cortices in patients with schizophrenia compared to the healthy subjects. In particular, the reduced rCBF in the left inferior prefrontal cortex accords with the structural changes observed in volumetric and DTI analyses in schizophrenic patients.

Structural abnormalities of the frontal cortex in schizophrenic patients have been suggested by many studies of MR volumetric images (reviewed in Honea et al., 2005; Glahn et al., 2008) and DTI (reviewed in Ellison-Wright and Bullmore, 2009). Altered function in the frontal cortex in schizophrenia has also been reported by functional MR imaging (fMRI) studies (e.g., Cannon et al., 2005; Ragland et al., 2005) and ASL studies (Scheef et al., 2010; Pinkham et al., 2011; Walther et al., 2011). In addition, other studies using SPECT found that patients with schizophrenia have decreased rCBF, particularly in the frontal lobes and/or left hemisphere (Weinberger et al., 1988; Andreasen et al., 1992; Vita et al., 1995; Kanahara et al., 2009).

In the present study, we found abnormalities in the inferior prefrontal region of the schizophrenic patients by volumetric imaging, DTI, and pCASL with partial volume effect correction, and these results are compatible with the above-mentioned previous findings. Longitudinal MRI studies suggested a progressive loss of prefrontal gray matter in schizophrenia (Sporn et al., 2003; Ota et al., 2009). Inferior prefrontal cortex was associated with the performance in cognitive switching by the MRI volume study (Ohtani et al., 2014). A volume and functional MRI study also supported that deficits in default mode network deactivation explained by the left inferior frontal gyrus thinning are related to impaired executive function in schizophrenia (Pujol et al., 2013). It is also known that the severity of schizophrenic negative symptoms is well correlated with the hypoactivity of the inferior prefrontal region and bilateral superior temporal regions (Pinkham et al., 2011), and these detections were compatible with our results that showed a nominal correlation between PANSS negative scale and rCBF in bilateral superior temporal gyri and left inferior prefrontal region. Since the majority of our patients were chronic cases, the observed brain change in the inferior prefrontal region may have arisen due, in part, to the progressive change and symptomatological change.

ASL studies of schizophrenia revealed several rCBF changes (Horn et al., 2009; Scheef et al., 2010; Pinkham et al., 2011; Walther et al., 2011). As shown in Table 3, the results of these studies differ substantially. For the frontal cortex, however, three of these four studies reported reduced rCBF, which is compatible with our results. We found rCBF reduction in bilateral occipital cortices of the individuals with schizophrenia, which is consistent with the study by Pinkham et al. (2011) in medicated schizophrenic patients and the study by Scheef et al. (2010) in drug-free subjects. Several studies obtained evidence of deficits of schizophrenia in visual processing, using electroencephalography (EEG) (Butler et al., 2001, 2005; Doniger et al., 2002), and other studies documented the abnormal EEG activities in the occipital lobe of patients with schizophrenia (Spencer et al., 2003, 2004). Neuroimaging studies of schizophrenia also revealed the decrease of white matter integrity in occipital white matter adjacent to the splenium of the corpus callosum that may originate in visual perception area (Agartz et al., 2001; Ardekani et al., 2003; Butler et al., 2005). Butler et al., detected the relationship between the evoked potential deficits and white matter intensity in the optic radiations (2005). Thus, it seems likely that the occipital lobe is involved in some aspects of the pathophysiology of schizophrenia. For other brain regions, previous studies pointed to reduced rCBF in temporal and parietal regions (Vita et al., 1995; Kanahara et al., 2009). The discrepancy between the previous results and ours may be attributable, at least in part, to the different methodology used for the ASL, particularly our study's consideration of the partial volume effect. Since this is the first ASL study that took this effect into account, further studies are necessary to draw any conclusion regarding rCBF changes in schizophrenia beyond structural brain changes.

In conclusion, our pCASL study with partial volume effect correction together with the volumetry and DTI data demonstrated hypoactivity in the left prefrontal area beyond structural abnormalities in schizophrenia patients. There were also hypofunction areas in bilateral occipital cortices, although the accompanying structural abnormalities were not apparent. Further studies are warranted to delineate the rCBF

Table 2
Differences of cerebral blood flow between schizophrenia patients and healthy volunteers in the inferior frontal gyri.

	x	y	z	Cluster size	FWE *p*	Z score
Inferior frontal gyri	−52	44	−8	10	0.022	3.98

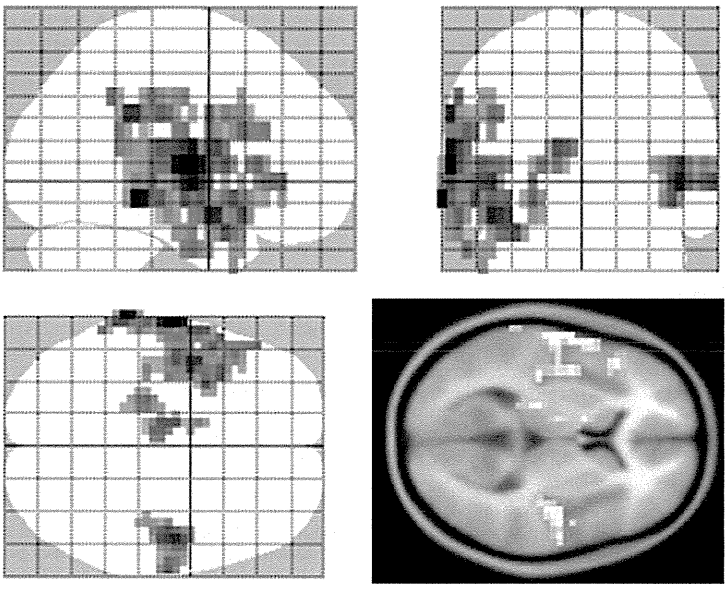

Fig. 3. Correlations between rCBF and symptomatology. There were no significant correlations between rCBF and PANSS subscales, however we found a nominal negative correlation between PANSS negative scale and rCBF in bilateral superior temporal gyri, left inferior prefrontal cortex, and left thalamus at trend level ($p = 0.006$).

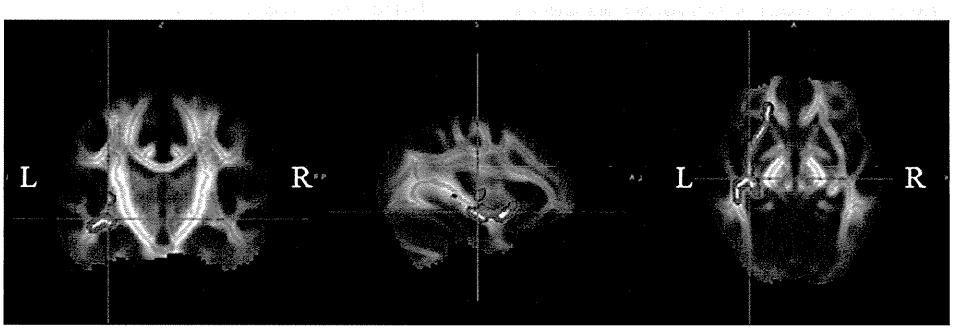

Fig. 4. Anisotropic changes in schizophrenia. There were significant reductions of fractional anisotropy (FA) in the left superior temporal region, left external capsule, and left inferior frontal region of the patients with schizophrenia (threshold-free cluster enhancement [TFCE], $p < 0.05$ family-wise error [FWE]). The background image is the standard MNI152 brain template. Green voxels represent the FA white matter skeleton.

changes in schizophrenia based on ASL. Consideration of the partial volume effect might be an important factor in evaluations of rCBF using ASL.

Role of the funding source

The funding source had no involvement.

Contributors

Miho Ota designed the study and wrote the first draft of the manuscript.
Masanori Ishikawa collected data.
Noriko Sato managed the analyses.
Mitsutoshi Okazaki collected data.
Norihide Maikusa brushed up the method of processing MRI data.
Hiroaki Hori collected data.
Kotaro Hattori collected data.
Toshiya Teraishi collected data.
Kimiteru Ito collected data.
Hiroshi Kunugi managed the analyses.
All authors contributed to and have approved the final manuscript.

Conflict of interest

All authors declare that they have no conflicts of interest.

Table 3
Overview of regional cerebral blood flow changes in patients with schizophrenia using arterial spin labeling.

Study	Subjects	Findings patients < control	Findings patients > control
Horn et al. (2009)	13 Patients with schizophrenia and 13 healthy controls	None	None
Pinkham et al. (2011)	30 Patients with schizophrenia and 24 healthy controls	Left frontal lobe, bilateral occipital lobes, and bilateral parietal lobes	Left putamen/superior corona radiata and right middle temporal lobes
Scheef et al. (2010)	11 Nonmedicated patients with schizophrenia and 25 healthy controls	Bilateral frontal lobes, bilateral parietal lobes, bilateral temporal lobes, and left cuneus	Cerebellum, brainstem, and thalamus
Walther et al. (2011)	11 Patients with schizophrenia and 14 healthy controls	Right prefrontal lobe, left temporal lobe, left parahippocampal gyrus, and right thalamus.	None

Please cite this article as: Ota, M., et al., Pseudo-continuous arterial spin labeling MRI study of schizophrenic patients, Schizophr. Res. (2014), http://dx.doi.org/10.1016/j.schres.2014.01.035

Acknowledgment

This study was supported by the Health and Labor Sciences Research Grants (Comprehensive Research on Disability, Health, and Welfare) (M.O. and H.K.), the Intramural Research Grant (24–11) for Neurological and Psychiatric Disorders of NCNP (M.O. and H.K.), "Understanding of molecular and environmental bases for brain health" carried out under the Strategic Research Program for Brain Sciences by the Ministry of Education, Culture, Sports, Science and Technology of Japan (H.K.).

References

Agartz, I., Andersson, J.L., Skare, S., 2001. Abnormal brain white matter in schizophrenia: a diffusion tensor imaging study. Neuroreport 12 (10), 2251–2254.

American Psychiatric Association, 1994. DSM-IV: Diagnostic and Statistical Manual of Mental Disorders, 4th ed. American Psychiatric Press, Washington, DC, Washington, DC.

American Psychiatric Association, 1997. Practice Guidelines for the Treatment of Patients with Schizophrenia. American Psychiatric Press, Washington, DC, Washington, DC.

Andreasen, N.C., Rezai, K., Alliger, R., Swayze, V.W., Flaum, M., Kirchner, P., Cohen, G., O'Leary, D.S., 1992. Hypofrontality in neuroleptic-naive patients and in patients with chronic schizophrenia. Assessment with xenon 133 single-photon emission computed tomography and the Tower of London. Arch. Gen. Psychiatry 49 (12), 943–958.

Ardekani, B.A., Nierenberg, J., Hoptman, M.J., Javitt, D.C., Lim, K.O., 2003. MRI study of white matter diffusion anisotropy in schizophrenia. Neuroreport 14 (16), 2025–2029.

Ashburner, J., 2007. A fast diffeomorphic image registration algorithm. NeuroImage 38 (1), 95–113.

Aslan, S., Xu, F., Wang, P.L., Uh, J., Yezhuvath, U.S., van Osch, M., Lu, H., 2010. Estimation of labeling efficiency in pseudocontinuous arterial spin labeling. Magn. Reson. Med. 63 (3), 765–771.

Butler, P.D., Schechter, I., Zemon, V., Schwartz, S.G., Greenstein, V.C., Gordon, J., Schroeder, C.E., Javitt, D.C., 2001. Dysfunction of early-stage visual processing in schizophrenia. Am. J. Psychiatry 158 (7), 1126–1133.

Butler, P.D., Zemon, V., Schechter, I., Saperstein, A.M., Hoptman, M.J., Lim, K.O., Revheim, N., Silipo, G., Javitt, D.C., 2005. Early-stage visual processing and cortical amplification deficits in schizophrenia. Arch. Gen. Psychiatry 62 (5), 495–504.

Cannon, T.D., Glahn, D.C., Kim, J., Van Erp, T.G., Karlsgodt, K., Cohen, M.S., Nuechterlein, K.H., Bava, S., Shirinyan, D., 2005. Dorsolateral prefrontal cortex activity during maintenance and manipulation of information in working memory in patients with schizophrenia. Arch. Gen. Psychiatry 62 (10), 1071–1080.

Casanova, R., Srikanth, R., Baer, A., Laurienti, P.J., Burdette, J.H., Hayasaka, S., Flowers, L., Wood, F., Maldjian, J.A., 2007. Biological parametric mapping: a statistical toolbox for multimodality brain image analysis. NeuroImage 34 (1), 137–143.

Cavuşoğlu, M., Pfeuffer, J., Uğurbil, K., Uludağ, K., 2009. Comparison of pulsed arterial spin labeling encoding schemes and absolute perfusion quantification. Magn. Reson. Imaging 27 (8), 1039–1045.

Doniger, G.M., Foxe, J.J., Murray, M.M., Higgins, B.A., Javitt, D.C., 2002. Impaired visual object recognition and dorsal/ventral stream interaction in schizophrenia. Arch. Gen. Psychiatry 59 (11), 1011–1020.

Ellison-Wright, I., Bullmore, E., 2009. Meta-analysis of diffusion tensor imaging studies in schizophrenia. Schizophr. Res. 108 (1–3), 3–10.

Glahn, D.C., Laird, A.R., Ellison-Wright, I., Thelen, S.M., Robinson, J.L., Lancaster, J.L., Bullmore, E., Fox, P.T., 2008. Meta-analysis of gray matter anomalies in schizophrenia: application of anatomic likelihood estimation and network analysis. Biol. Psychiatry 64 (9), 774–781.

Honea, R., Crow, T.J., Passingham, D., Mackay, C.E., 2005. Regional deficits in brain volume in schizophrenia: a meta-analysis of voxel-based morphometry studies. Am. J. Psychiatry 162 (12), 2233–2245.

Horn, H., Federspiel, A., Wirth, M., Müller, T.J., Wiest, R., Wang, J.J., Strik, W., 2009. Structural and metabolic changes in language areas linked to formal thought disorder. Br. J. Psychiatry 194 (2), 130–138.

Inagaki, A., Inada, T., Fujii, Y., Yagi, G., 1999. Equivalent Dose of Psychotropics. Seiwa Shoten, Tokyo.

Kanaan, R.A., Kim, J.S., Kaufmann, W.E., Pearlson, G.D., Barker, G.J., McGuire, P.K., 2005. Diffusion tensor imaging in schizophrenia. Biol. Psychiatry 58 (12), 921–929.

Kanahara, N., Shimizu, E., Sekine, Y., Uchida, Y., Shibuya, T., Yamanaka, H., Hashimoto, T., Asaka, T., Sasaki, T., Miyatake, R., Ohkami, T., Fukami, G., Fujisaki, M., Watanabe, H., Shirayama, Y., Hayashi, H., Hashimoto, K., Asano, M., Iyo, M., 2009. Does hypofrontality expand to global brain area in progression of schizophrenia? A cross-sectional study between first-episode and chronic schizophrenia. Prog. Neuropsychopharmacol. Biol. Psychiatry 33 (3), 410–415.

Kay, S.R., Opler, L.A., Fiszbein, A., 1987. Positive and Negative Syndrome Scale (PANSS) manual. Schizophr. Bull. 13 (2), 261–276.

Kubicki, M., McCarley, R., Westin, C.F., Park, H.J., Maier, S., Kikinis, R., Jolesz, F.A., Sheoton, M.E., 2007. A review of diffusion tensor imaging studies in schizophrenia. J. Psychiatr. Res. 41 (1–2), 15–30.

Lu, H., Clingman, C., Golay, X., van Zijl, P.C., 2004. Determining the longitudinal relaxation time (T1) of blood at 3.0 Tesla. Magn. Reson. Med. 52 (3), 679–682.

Maldjian, J.A., Laurienti, P.J., Kraft, R.A., Burdette, J.H., 2003. An automated method for neuroanatomic and cytoarchitectonic atlas-based interrogation of fMRI data sets. NeuroImage 19 (3), 1233–1239.

Nichols, T.E., Holmes, A.P., 2002. Nonparametric permutation tests for functional neuroimaging: a primer with examples. Hum. Brain Mapp. 15 (1), 1–25.

Ohtani, T., Levitt, J.J., Nestor, P.G., Kawashima, T., Asami, T., Shenton, M.E., Niznikiewicz, M., McCarley, R.W., 2014. Prefrontal cortex volume deficit in schizophrenia: a new look using 3 T MRI with manual parcellation. Schizophr. Res. 152 (1), 184–190.

Ota, M., Obu, S., Sato, N., Mizukami, K., Asada, T., 2009. Progressive brain changes in schizophrenia: a one-year follow up study of diffusion tensor imaging. Acta Neuropsychiatr. 21, 301–307.

Ota, M., Sato, N., Nakata, Y., Ito, K., Kamiya, K., Maikusa, N., Ogawa, M., Okamoto, T., Obu, S., Noda, T., Araki, M., Yamamura, T., Kunugi, H., 2013. Abnormalities of cerebral blood flow in multiple sclerosis: a pseudo-continuous arterial spin labeling MRI study. Magn. Reson. Imaging 31, 990–995.

Otsubo, T., Tanaka, K., Koda, R., Shinoda, J., Sano, N., Tanaka, S., 2005. Reliability and validity of Japanese version of the Mini-International Neuropsychiatric Interview. Psychiatry Clin. Neurosci. 59 (5), 517–526.

Pinkham, A., Loughead, J., Ruparel, K., Wu, W.C., Overton, E., Gur, R., Gur, R., 2011. Resting quantitative cerebral blood flow in schizophrenia measured by pulsed arterial spin labeling perfusion MRI. Psychiatry Res. 194 (1), 64–72.

Pujol, N., Penadés, R., Rametti, G., Catalán, R., Vidal-Piñeiro, D., Palacios, E., Bargallo, N., Bernardo, M., Junqué, C., 2013. Inferior frontal and insular cortical thinning is related to dysfunctional brain activation/deactivation during working memory task in schizophrenic patients. Psychiatry Res. 214 (2), 94–101.

Ragland, J.D., Gur, R.C., Valdez, J.N., Loughead, J., Elliott, M., Kohler, C., Kanes, S., Siegel, S.J., Moelter, S.T., Gur, R.E., 2005. Levels-of-processing effect on frontotemporal function in schizophrenia during word encoding and recognition. Am. J. Psychiatry 162 (10), 1840–1848.

Scheef, L., Manka, C., Daamen, M., Kühn, K.U., Maier, W., Schild, H.H., Jessen, F., 2010. Resting-state perfusion in nonmedicated schizophrenic patients: a continuous arterial spin-labeling 3.0-T MR study. Radiology 256 (1), 253–260.

Sheehan, D.V., Lecrubier, Y., Sheehan, K.H., Amorim, P., Janavs, J., Weiller, E., Hergueta, T., Baker, R., Dunbar, G.C., 1998. The Mini-International Neuropsychiatric Interview (M.I.N.I.): the development and validation of a structured diagnostic psychiatric interview for DSM-IV and ICD-10. J. Clin. Psychiatry 59, 22–57.

Shenton, M.E., Dickey, C.C., Frumin, M., McCarley, R.W., 2001. A review of MRI findings in schizophrenia. Schizophr. Res. 49 (1–2), 1–52.

Smith, S.M., Jenkinson, M., Johansen-Berg, H., Rueckert, D., Nichols, T.E., Mackay, C.E., Watkins, K.E., Ciccarelli, O., Cader, M.Z., Matthews, P.M., Behrens, T.E., 2006. Tract-based spatial statistics: voxelwise analysis of multi-subject diffusion data. NeuroImage 31 (4), 1487–1505.

Smith, S.M., Jenkinson, M., Woolrich, M.W., Beckmann, C.F., Behrens, T.E., Johansen-Berg, H., Bannister, P.R., De Luca, M., Drobnjak, I., Flitney, D.E., Niazy, R.K., Saunders, J., Vickers, J., Zhang, Y., De Stefano, N., Brady, J.M., Matthews, P.M., 2004. Advances in functional and structural MR image analysis and implementation as FSL. NeuroImage 23 (Suppl. 1), S208–S219.

Smith, S.M., Nichols, T.E., 2009. Threshold-free cluster enhancement: addressing problems of smoothing, threshold dependence and localisation in cluster inference. NeuroImage 44 (1), 83–98.

Spencer, K.M., Nestor, P.G., Niznikiewicz, M.A., Salisbury, D.F., Shenton, M.E., McCarley, R.W., 2003. Abnormal neural synchrony in schizophrenia. J. Neurosci. 23 (19), 7407–7411.

Spencer, K.M., Nestor, P.G., Perlmutter, R., Niznikiewicz, M.A., Klump, M.C., Frumin, M., Shenton, M.E., McCarley, R.W., 2004. Neural synchrony indexes disordered perception and cognition in schizophrenia. Proc. Natl. Acad. Sci. U. S. A. 101 (49), 17288–17293.

Sporn, A.L., Greenstein, D.K., Gogtay, N., Jeffries, N.O., Lenane, M., Gochman, P., Clasen, L.S., Blumenthal, J., Giedd, J.N., Rapoport, J.L., 2003. Progressive brain volume loss during adolescence in childhood-onset schizophrenia. Am. J. Psychiatry 160 (12), 2181–2189.

Tzourio-Mazoyer, N., Landeau, B., Papathanassiou, D., Crivello, F., Etard, O., Delcroix, N., Mazoyer, B., Joliot, M., 2002. Automated anatomical labeling of activations in SPM using a macroscopic anatomical parcellation of the MNI MRI single-subject brain. NeuroImage 15 (1), 273–289.

Vita, A., Bressi, S., Perani, D., Invernizzi, G., Giobbio, G.M., Dieci, M., Garbarini, M., Del Sole, A., Fazio, F., 1995. High-resolution SPECT study of regional cerebral blood flow in drug-free and drug-naive schizophrenic patients. Am. J. Psychiatry 152 (6), 876–882.

Walther, S., Federspiel, A., Horn, H., Razavi, N., Wiest, R., Dierks, T., Strik, W., Müller, T.J., 2011. Resting state cerebral blood flow and objective motor activity reveal basal ganglia dysfunction in schizophrenia. Psychiatry Res. 192 (2), 117–124.

Wang, J., Zhang, Y., Wolf, R.L., Roc, A.C., Alsop, D.C., Detre, J.A., 2005. Amplitude-modulated continuous arterial spin-labeling 3.0-T perfusion MR imaging with a single coil: feasibility study. Radiology 235 (1), 218–228.

Wang, Z., Aguirre, G.K., Rao, H., Wang, J., Fernández-Seara, M.A., Childress, A.R., Detre, J.A., 2008. Empirical optimization of ASL data analysis using an ASL data processing toolbox: ASLtbx. Magn. Reson. Imaging 26 (2), 261–269.

Weinberger, D.R., Berman, K.F., Illowsky, B.P., 1988. Physiological dysfunction of dorsolateral prefrontal cortex in schizophrenia. III. A new cohort and evidence for a monoaminergic mechanism. Arch. Gen. Psychiatry 45 (7), 609–615.

Please cite this article as: Ota, M., et al., Pseudo-continuous arterial spin labeling MRI study of schizophrenic patients, Schizophr. Res. (2014), http://dx.doi.org/10.1016/j.schres.2014.01.035